KEKセミナー　　2004.5.7/5.28
「高エネルギー物理学と宇宙像」

重力波実験と精密重力実験 その四

東京大学宇宙線研究所
黒田和明

Content

- Brief comments on time variation of G
- Motivation of the measurements
- Millimeter scale experiment

Motivation of the measurements

- Scalar Tensor Theory by Fujii

  $\phi(r) \propto [\,1 + \alpha\, e^{-r/\lambda}\,]/r \qquad \alpha = 2/3,\ \lambda \sim 1\mathrm{km}$
- Empirical speculation by Long (1976)

  $G \propto 1 + \varepsilon \ln r(\mathrm{cm}) \qquad \varepsilon = 0.002 \pm 0.0004$
- Related to the fifth force (scalar+vector fields)

  $\phi(r) \propto [\,1 + a\, e^{-ar} + b\, e^{-br}\,]/r$
- Extra-dimension

Extra Dimension

- String theory---long-sought unified description of the four forces of nature and elementary particles
- Six extra spatial dimensions beyond the three required
- These extra dimensions are curled up into small spaces---compactification induces “moduli” fields
- Moduli fields generates forces with strengths comparable to gravity→ J.C.Long et al (Nature 421, 922, 2003)
- Other theoretical outcome →string dilaton, axion

Measurement summary

- C.D.Hoyle et al., Phys. Rev. Lett. 86, 1418, 2001
- J. C. Long et al., Nature 421, 922, 2003
- J. Chiaverini, et al., Phys. Rev. Lett. 90, 151101-1, 2003

J.D. Hoyle et al.
Washington University

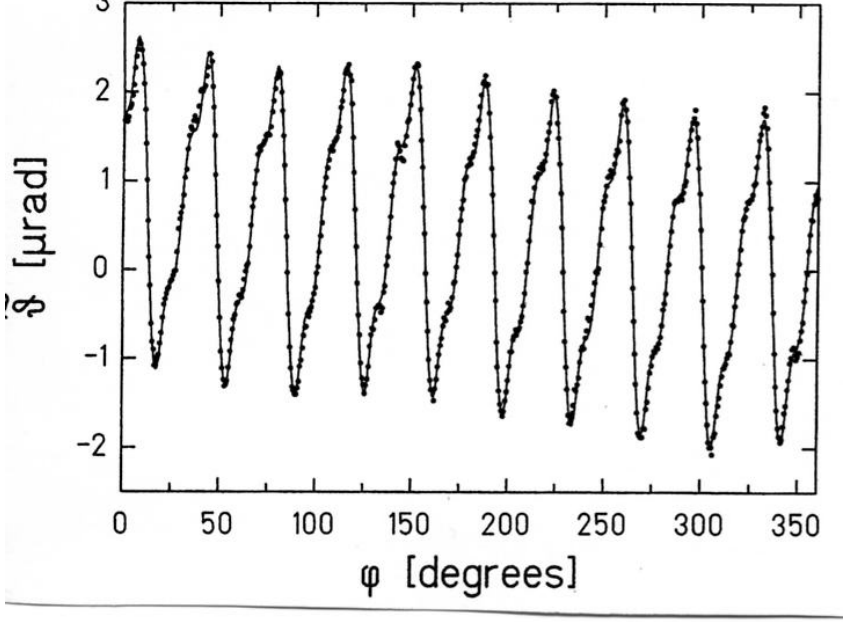

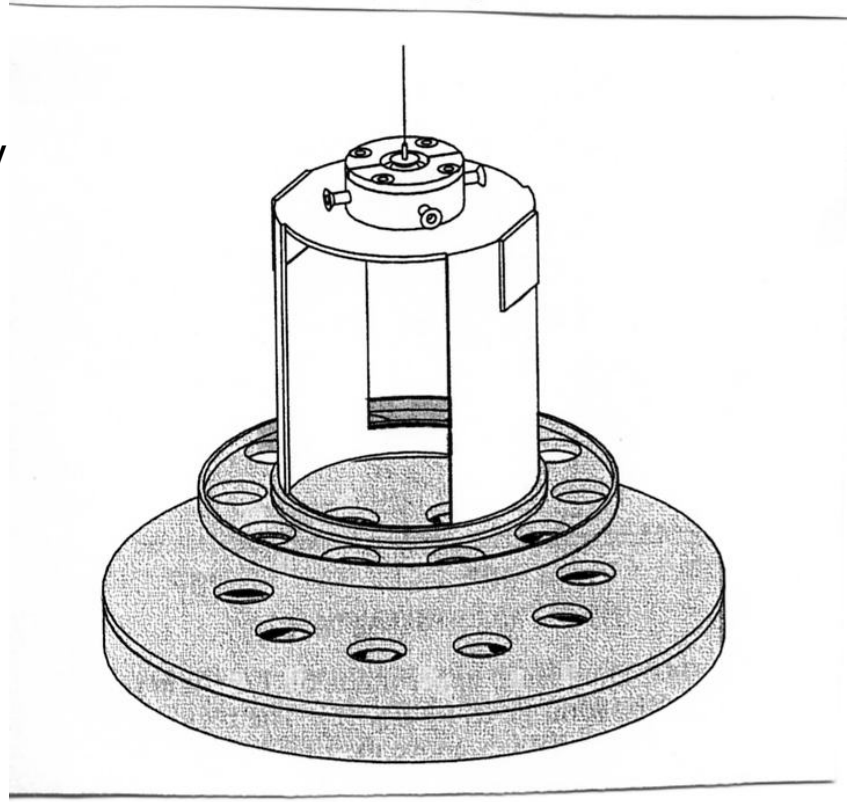

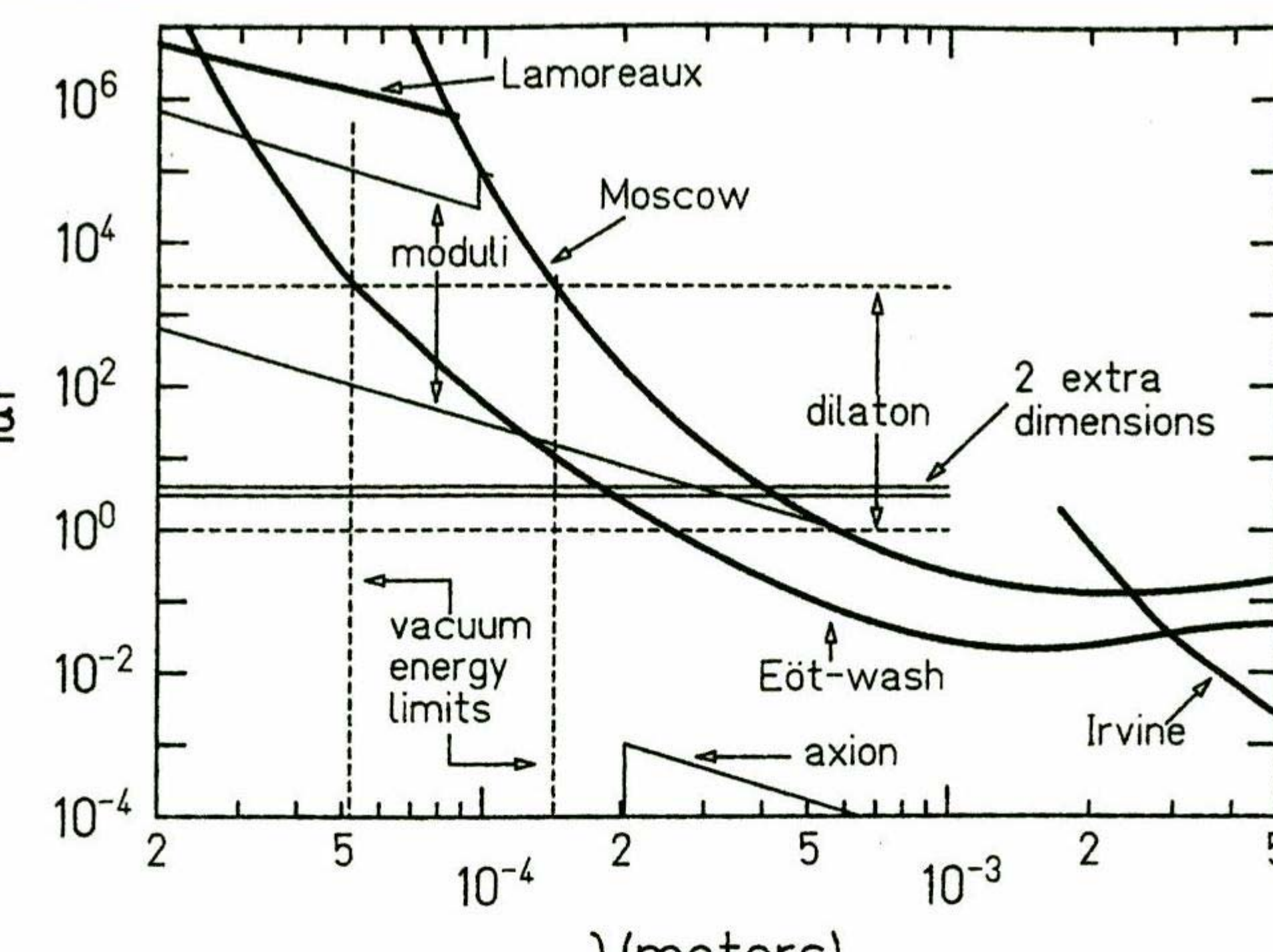
Lamoreaux
Moscow
moduli
dilaton
2 extra dimensions
vacuum energy limits
Eöt-wash
Irvine
axion
10^6
10^4
10^2
10^0
10^{-2}
10^{-4}
2
5
10^{-4}
2
5
10^{-3}
2

J.C.Long, et al, Nature 421, 922 (2003)

leading to λ in the centimetre to micrometre range. In the strange and gluon moduli case, M is the scale where supersymmetry breaking occurs, whereas in the radion modulus case it corresponds to the size of one or more compact dimensions. This formula also applies to the ADD theory[14] (named for its authors) in which two

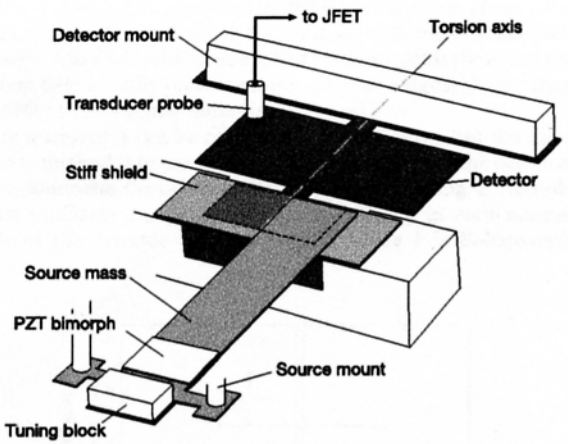

Figure 1 Major components of the apparatus. The smaller rectangle of the tungsten detector (under the shield) is 11.455 mm wide, 5.080 mm long and 195 μm thick. The detector is annealed at 1,300 °C to increase its mechanical Q to 25,000. In operation the 1,173.085-Hz resonant frequency of the detector is stabilized by actively controlling the detector temperature to 305 K. The tungsten source mass is 35 mm long, 7 mm wide and 305 μm thick. The source mass resonant frequency is tuned to the detector and driven by the PZT (lead zirconate titanate) piezoelectric bimorph. The shield is a 60-μm-thick sapphire plate coated with 100 nm of gold on both sides. The test masses and the shield are supported by three separate five-stage passive vibration isolation stacks[23], each providing approximately 200-dB attenuation at 1 kHz. Mechanical probes are used to directly measure the relative orientation and position of each component, and to measure the source mass amplitude. Detector motions are sensed by a cylindrical capacitive probe supported 100 μm above a rear corner of the large rectangle of the detector mass. The probe is biased at 200 V through a 100 GΩ resistor, and connected to an SK 152 junction field-effect transistor (JFET) through a blocking capacitor. The JFET noise temperature of 100 mK is more than sufficient to detect 305 K thermal motions of the detector mass. The JFET preamplifier is followed by a second preamplifier, filters, and finally a two-phase lock-in amplifier. The total voltage gain from the capacitive probe to the lock-in input is approximately 1600. A crystal-controlled oscillator provides a reference signal for the lock-in amplifier and drives the source mass PZT through a 1:10 step-up transformer.

lock-in amplifier. To suppress background forces due to electrostatics and residual gas, a stiff conducting shield is fixed between the test masses. With the source at rest, the gap between source and detector is adjusted to 108 μm, and the entire apparatus is placed in a vacuum enclosure and maintained at pressures below 2×10^{-7} torr.

Figure 2 shows histograms of the raw data, collected with the source mass drive tuned both on and off the detector resonant frequency. Each plot contains data from one channel of the lock-in amplifier, corresponding to one of two orthogonal phases of the

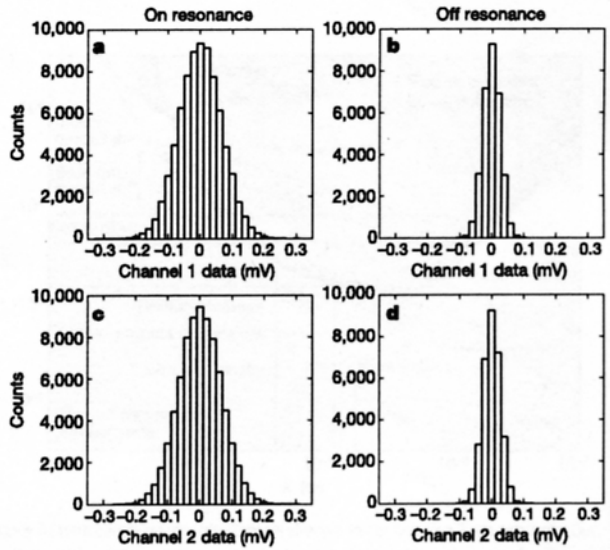

Figure 2 Distributions of data samples. Data were recorded at 1 Hz with a lock-in bandwidth chosen to include the noise power of the detector thermal oscillations, which was used for calibration. Each data cycle began with five 120-sample diagnostic runs with a direct-current bias of 5–10 V applied to the shield to induce a large test force, transmitted from source to detector via deflections of the shield. The biased runs were recorded at five drive frequencies separated by 15 mHz to cover the detector resonance. The shield was then grounded and the cycle continued with 720 samples with the drive tuned on-resonance (**a**, **c**) and 288 samples with the drive tuned 2 Hz below the detector resonance (**b**, **d**). The off-resonance run provided a continuous zero check. A total of 108 such cycles were acquired over five days yielding 77,760 on-resonance samples. The biased diagnostic data show that the source mass amplitude, the detector Q and resonant frequency, and the electronic gain were all stable throughout the data set.

ally present cannot generate a signal greater than
ermal-noise-limited sensitivity.
can be calibrated in several ways, but the most
s to use the r.m.s. thermal motion of the detector,
he on-resonance distributions in Fig. 2. Accord-
on, the average kinetic energy in each normal
ctor is equal to $\frac{1}{2}kT$, where k is Boltzmann's

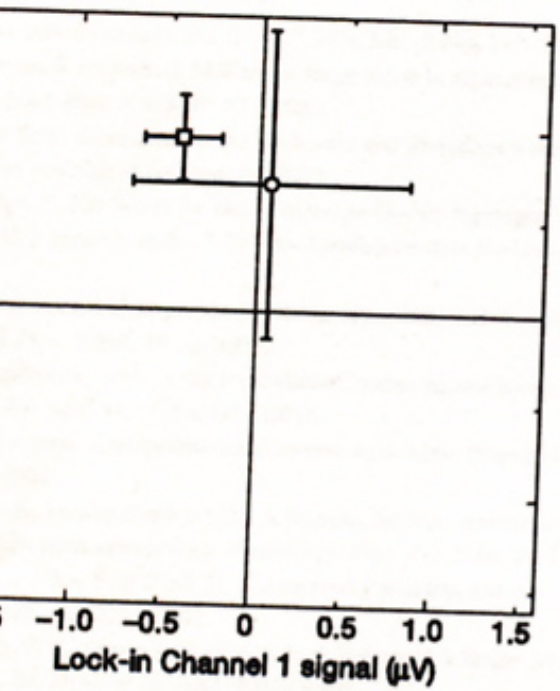

and on-resonance data samples. The circular point with the
s the on-resonance mean. Correlations between nearby
ted for in computing the standard deviations shown by error
he origin is due to leakage of the reference signal internal to
ith the shield removed and a bias voltage between the source
hase for an attractive force is 189°. The on-resonance mean
an at 189° is −0.44 ± 0.89

an upper limit on λ of 88 μm, close to the value of 40 μm estimated

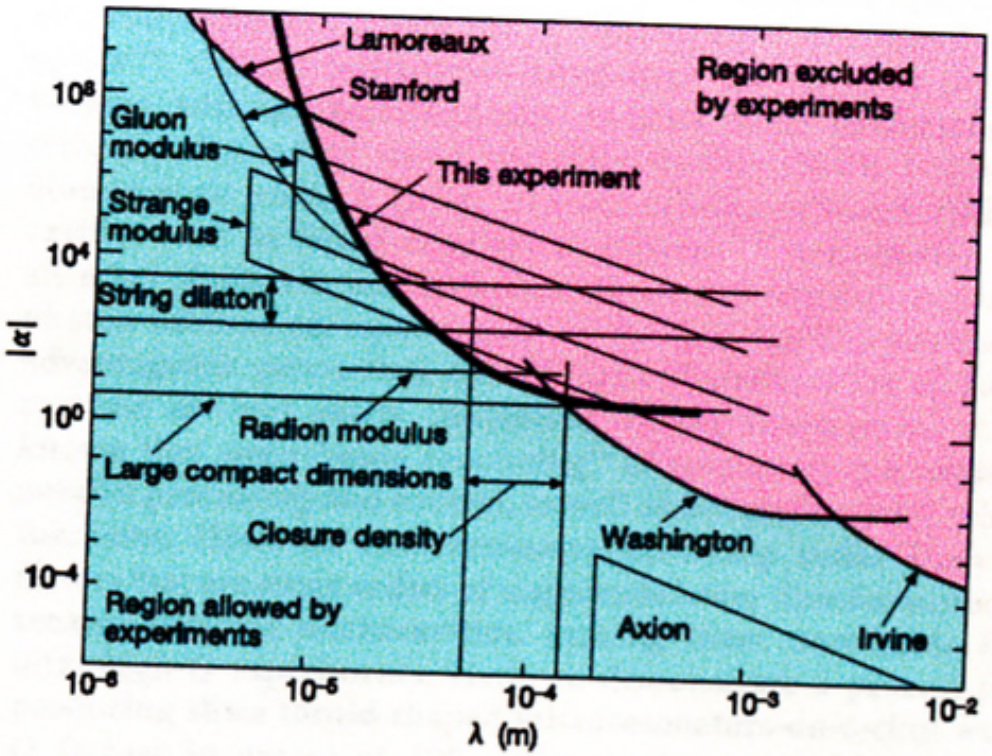

Figure 4 Current limits on new gravitational strength forces between 1 μm and 1 cm. Our result is a 95% confidence-level upper limit on the Yukawa strength α as a function of range λ (solid bold curve). It is shown together with limits from previous experiments (Lamoreaux[24], Washington[12], Irvine[25]) and theoretical predictions newly constrained (gluon modulus[4], strange modulus[4], string dilaton[2], radion modulus[7]). An unpublished limit from the Stanford experiment[26] is also shown; it is derived in the presence of a background force. The dilaton strength is somewhat model-dependent and there is a range of values reported in the literature[2]. We have chosen the region $200 < \alpha < 3{,}000$, which includes most values. Also shown are predictions from the ADD theory with two large compact extra dimensions[14,27,28], axion mediated forces[20,21]

the actuator's motion was measured capacitively [illegible] calibration obtained from this initial characterization. The actuator's drive frequency was tuned to one-third of the cantilever resonant frequency by means of magnetic excitation. The amplitude of actuator motion was 98 ±

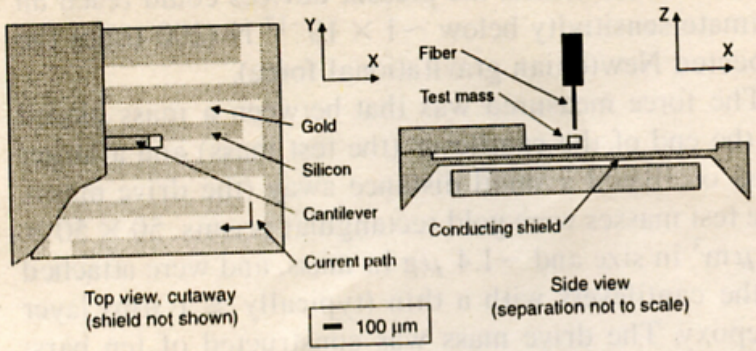

FIG. 1. Schematic top and side views of test mass on cantilever and drive mass below, showing alternating gold and silicon drive mass bars. Drive mass motion was in the Y direction.

means of direct mechanical contact (sensed by the cantilever) between the drive mass and the shield. Subsequent motion away from the shield was measured with the CPS, and the separation between the masses was thus known to an accuracy of 2 μm.

The cantilever, actuator, and vibration isolation stages were suspended in a vacuum can at the end of a probe that was inserted into a liquid helium research dewar. An exchange gas space separated the inner vacuum can from the liquid helium in order to reduce external vibrations due to helium boiloff. The entire system was supported by 2 m long ~2 Hz springs for additional isolation. The experiments were performed at $T = 9$–11 K and at gas pressures of less than 10^{-4} torr (room temperature reading) with further cryopumping while cold.

The sinusoidal actuator voltage and the cantilever displacement signal were sampled and stored simultaneously at 10 kHz using an analog-to-digital converter. The displacement data stream was then sorted into bins using the

J. Chiaverini, et al., Phys. Rev. Lett. 90, 151101-1 (2003)

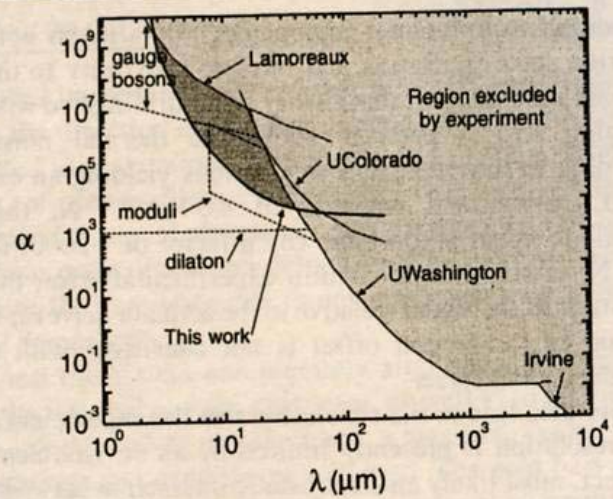

FIG. 4. Strength versus length scale parameter space [see Eq. (1)] for non-Newtonian effects showing area excluded by present (darker shaded region bounded by signal plus 2σ-level error) and previous (lighter shaded region) experiments. Lines labeled Lamoreaux, UWashington, UColorado, and Irvine are from [12], [2], [13], and [14], respectively. Theoretical predictions (dashed lines) are adapted from [15,4] (dilaton and moduli) and from [1,16] (gauge bosons).

motion of the shield, the oscillatory force is on the order of 1×10^{-21} N, much less than the thermal noise of the cantilever for experimental measurement times.

The motion of the membrane could also induce can-

is an important one, as it contains previously unexplored space for scalar moduli particles.

We have presented results from a search for gravitylike deviations from Newtonian theory at distance scales below 100 μm using a microcantilever approach, with masses of size on the order of these scales. Our data offer a new limit on non-Newtonian effects in the range of 10 μm, constraining theoretical predictions of moduli.

We thank Thomas Kenny and Savas Dimopoulos for useful discussions. J. C. and D. M. W. thank DoD for support. S. J. S. thanks NSF for support. This work made use of the National Nanofabrication Users Network facilities supported by the National Science Foundation under Award No. ECS-9731294.

Note added.—After submission of this manuscript, results for larger length scales were published from a similar experiment at the University of Colorado [18].

[1] N. Arkani-Hamed, S. Dimopoulos, and G. Dvali, Phys. Rev. D **59**, 086004 (1999).
[2] C. D. Hoyle *et al.*, Phys. Rev. Lett. **86**, 1418 (2001).
[3] For a review, see, e.g., J. C. Long *et al.*, Nucl. Phys. **B539**, 23 (1999) or E. Fischbach *et al.*, Phys. Rev. D **64**, 075010 (2001).
[4] S. Dimopoulos and G. F. Giudice, Phys. Lett. B **379**, 105 (1996).
[5] D. Rugar, H. J. Mamin, and P. Guethner, Appl. Phys. Lett. **55**, 2588 (1989).

まとめ

- 微小距離でのニュートン重力を精密に計る実験に改善が見られる。
- 低温技術の適用など新しい手法が開発されている。
- ミリメータースケールよりも大きいスケールでこれまでにない精度を実現する方法もある。
- 余次元重力はまだ見つかっていない。